

The Analysis of the UKF-Based Navigation Algorithm during GPS Outage

V. Bistrovs¹, A. Kluga²

¹*Department of Transport Electronics and Telematics, Riga Technical University,
Lomonosova iela 1, V korpuss, LV-1019 Riga, Latvia
bistrov@inbox.lv*

²*Department of Transport Electronics and Telematics, Riga Technical University,
Lomonosova iela 1, V korpuss, LV-1019 Riga, Latvia
ansis.kluga@rtu.lv*

Abstract—The unscented Kalman filter (UKF) became very attractive for the navigation sensors data fusion, because of algorithm significant accuracy and implementation advantages. The unscented Kalman filter is based on the unscented transform (UT) to perform the estimation of the system states. The main idea of the unscented transformation is following. It's more effective to approximate probability distribution function than arbitrary transformation or nonlinear function.

The developed sensors data fusion algorithm using the UKF is considered in this work. This algorithm was applied for the state estimation of the loosely coupled GPS/INS integrated navigation system. GPS/INS integrated navigation system contains low cost inertial sensors and low cost GPS receiver. To demonstrate the estimation performance, the processing of sensors data was done using linear Kalman filter (KF), extended Kalman filter (EKF) and UKF. As a result, UKF has lower velocity estimation error than EKF during simulated GPS signal outage.

Index Terms—Unscented Kalman filter, GPS outage, microelectromechanical systems, inertial measurement unit.

I. INTRODUCTION

Nowadays, the data fusion from different sensors for the performance improving of the low cost integrated navigation system becomes necessary in the land vehicle navigation application. Core to the integrated navigation systems is the concept of fusing noisy measurements from GPS sensor, inertial measurement unit using nonlinear estimation techniques [1].

Modern MEMS technologies are offering light and low cost sensors. But measurements of MEMS sensors are less accurate and suffer from considerable noise level. The measurements are inaccurate and noisy because of sensor manufacturing technology itself and environmental effects such as mechanical vibrations and temperature. It's difficult to find simple and exact system model for such sensors [1], [2].

Currently, the most used technique to fuse the navigation data is the extended Kalman filter. Also, the linear Kalman filter can be used in some cases. Nonlinear estimation algorithms (which are based on the probabilistic approaches) are used for the GPS/IMU data fusion. The UKF can be

mentioned as one of the perspective nonlinear estimation algorithm for the land vehicle navigation for its accuracy and implementation advantages [3], [4].

The core of the UKF algorithm is the UT transformation. The UT was developed basing on idea that it is easier to approximate a probability distribution function of the analysed data using minimal set of the carefully selected samples [5], [6]. The UKF generates a set of specific points (sigma points) in such a way that this set approximates mean and covariance of the state and produces the estimation based on these points. The sigma points are propagated through true nonlinear equations of system model. The UT and the UKF have been introduced by Julier and Uhlmann [5], [6].

For the nonlinear system models and for the object of interest with not well defined system models, the UKF is potentially better solution than the EKF. The UKF has performance equivalent to the standard Kalman filter for linear systems and can be used for the state estimation of nonlinear systems without the linearization procedure required for the EKF.

The details of the developed data fusion algorithm for loosely coupled low cost integrated navigation system are discussed in Section II. In Section III, we focus on the practical application of the different data fusion techniques (KF, EKF and UKF) for the land vehicle velocity estimation during GPS signal outages. Also the results of performance analysis for KF, EKF and UKF are discussed.

II. SENSOR DATA PROCESSING ALGORITHM

The considered integrated navigation system consists of four sensors. These sensors are two MEMS accelerometers, one MEMS gyroscope and one position sensor (GPS). The inertial sensors were a part of self contained low cost IMU MotionNode. The position sensor was the low cost GPS receiver BU-353. The measurements of the sensors are saved onto HDD of notebook. Then measurement data is synchronized and processed by fusion algorithm.

The fusion algorithm of sensor data consists of the prediction and updating step. For the prediction step, we chose the frequency $f_2 = 50$ Hz. This frequency perfectly suits for our experiments, since the land vehicle is not

moving faster than 30 m/s. The frequency of the updating step is equal to the GPS output data rate $f_i = 1$ Hz. This GPS data is used to compensate measurement errors in the accelerometers and gyroscope readings. The algorithm block diagram is shown in Fig. 1.

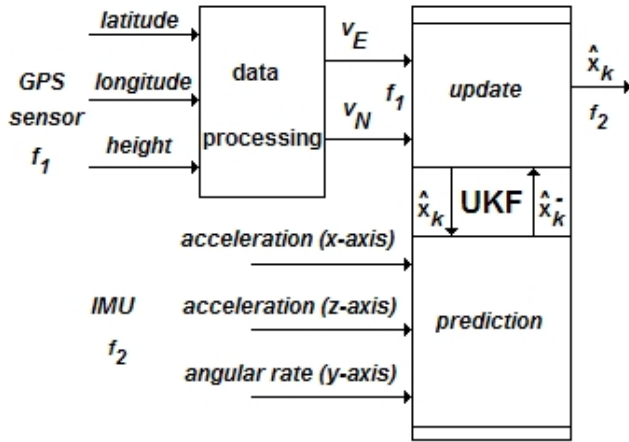


Fig. 1. The algorithm block diagram.

The navigation system state vector selected for the UKF is

$$\mathbf{x}_k = [b_{a_x} \ b_{a_z} \ a_x \ a_z \ v_x \ v_z \ b_{g_y} \ w_y \ \phi], \quad (1)$$

where b_{a_x} and b_{a_z} are the estimates of accelerometer biases, a_x and a_z are the estimates of acceleration along x-axis and z-axis, v_x and v_z are the estimates of velocities along x-axis and z-axis of vehicle coordinate frame, b_{g_y} is the estimate of gyroscope signal bias, w_y is the estimate of angular rate of vehicle around y-axis of vehicle coordinate frame, ϕ is the estimate of the heading of the vehicle. The orientation of the vehicle coordinate frame is shown in the Fig. 2. The longitudinal axis of the vehicle coordinate system is x. The lateral axis of the vehicle coordinate system is z, and the y-axis points downwards. The IMU is placed in the car in order the IMU x-axis and z-axis has the same orientation with the vehicle longitudinal and lateral axis.

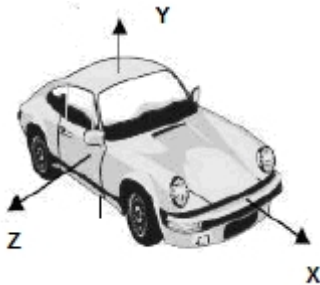


Fig. 2. The vehicle coordinate frame.

The navigation system state vector is propagated with the frequency $f_2 = 50$ Hz between measurements [7]:

$$\hat{b}_{a_x, i+1}^- = \beta_1 \cdot \hat{b}_{a_x, i}^- \quad (2)$$

$$\hat{b}_{a_z, i+1}^- = \beta_2 \cdot \hat{b}_{a_z, i}^- \quad (3)$$

$$\hat{b}_{w_y, i+1}^- = \beta_3 \cdot \hat{b}_{w_y, i}^- \quad (4)$$

$$\hat{a}_{x, i+1}^- = 0.5 \cdot (f_{x, i} + f_{x, i-1}) + \hat{b}_{a_x, i}^- \quad (5)$$

$$\hat{a}_{z, i+1}^- = 0.5 \cdot (f_{z, i} + f_{z, i-1}) + \hat{b}_{a_z, i}^- \quad (6)$$

$$\hat{w}_{y, i+1}^- = 0.5 \cdot (\phi_{y, i} + \phi_{y, i-1}) + \hat{b}_{w_y, i}^- \quad (7)$$

$$\hat{v}_{x, i+1}^- = \hat{v}_{x, i}^- + T \cdot \hat{a}_{x, i+1}^- \quad (8)$$

$$\hat{v}_{z, i+1}^- = \hat{v}_{z, i}^- + T \cdot \hat{a}_{z, i+1}^- \quad (9)$$

$$\hat{\phi}_{y, i+1}^- = \hat{\phi}_{y, i}^- + T \cdot \hat{w}_{y, i+1}^- \quad (10)$$

where $\beta_1, \beta_2, \beta_3$ are the fading factors; $f_{x, i}, f_{z, i}$ are the raw measurements of MEMS accelerometers, $\phi_{y, i}$ is the raw measurement of MEMS gyroscope, T is the sampling time. The values for the fading factors were determined experimentally during the process of adjusting algorithm parameters in order to guarantee acceptable performance of the algorithm i.e. minimal estimation error of the vehicle velocity. In most of the cases the fading factors were equal to 0.9999. These fading factors could be estimated more precisely using the linear prediction techniques.

The navigation system measurement vector is

$$\mathbf{y}_k = [v_N \ v_E], \quad (11)$$

where v_E is the east component of the vehicle velocity, v_N - is the north component of the vehicle velocity.

The observation model is given by the following nonlinear equations:

$$\hat{v}_{N, k} = \sqrt{[(\hat{v}_{x, k}^-)^2 + (\hat{v}_{z, k}^-)^2]} \cdot \cos(\hat{\phi}_{y, k}^-), \quad (12)$$

$$\hat{v}_{E, k} = \sqrt{[(\hat{v}_{x, k}^-)^2 + (\hat{v}_{z, k}^-)^2]} \cdot \sin(\hat{\phi}_{y, k}^-). \quad (13)$$

These nonlinear equations are directly used in the UKF algorithm.

The UKF procedure [5], [6] begins with the calculation of $2n + 1$ sigma points χ_{k-1} with a mean of $\hat{\mathbf{x}}_{k-1}$ and its covariance \mathbf{P}_{k-1}

$$\chi_{k-1} = [\hat{\mathbf{x}}_{k-1} \ \hat{\mathbf{x}}_{k-1} + \gamma \sqrt{\mathbf{P}_{k-1}} \ \hat{\mathbf{x}}_{k-1} - \gamma \sqrt{\mathbf{P}_{k-1}}], \quad (14)$$

where γ is the scaling parameter, which defines the distribution of the sigma points (SPs), and $k \in \{1, \dots, \infty\}$. Next step of the UKF process is transforming of each sigma point by use of the system dynamics

$$\chi_{k|k-1}^* = \mathbf{F}[\chi_{k-1}]. \quad (15)$$

Then compute the mean and covariance from the transformed SPs:

$$\hat{\mathbf{x}}_k^- = \sum_{i=0}^{2L} W_i^{(m)} \chi_{i, k|k-1}^* \quad (16)$$

$$\mathbf{P}_k^- = \sum_{i=0}^{2L} W_i^{(c)} [\chi_{i,k|k-1}^* - \hat{\mathbf{x}}_k^-][\chi_{i,k|k-1}^* - \hat{\mathbf{x}}_k^-]^T + \mathbf{Q}, \quad (17)$$

where \mathbf{Q} is the process noise covariance matrix. \mathbf{Q} is the diagonal matrix with the elements, defined using the technical data sheet for the sensors used in the considered integrated navigation system and adjusted during the algorithm runs in order to obtain the best performance of the algorithm. $W_i^{(m)}$ and $W_i^{(c)}$ is a set of the scalar weights. The weights are calculated as follows:

$$\begin{cases} W_0^{(m)} = \gamma^2 / (L + \gamma^2), \\ W_0^{(c)} = W_0^{(m)} + \alpha, \\ W_i^{(m)} = W_i^{(c)} / (2 \cdot (L + \gamma^2)), \end{cases} \quad (18)$$

where α is the secondary scaling parameter. This parameter was set to zero during adjusting scaling factor γ for guarantying positive definite of the covariance matrix \mathbf{P}_k during all iteration steps of the algorithm.

After that we have to define a new set of SPs to incorporate the effect of the additive noise [6]

$$\chi_{k|k-1} = [\hat{\mathbf{x}}_k^- \quad \hat{\mathbf{x}}_k^- + \gamma\sqrt{\mathbf{P}_k^-} \quad \hat{\mathbf{x}}_k^- - \gamma\sqrt{\mathbf{P}_k^-}]. \quad (19)$$

Then the SPs are transformed through the measurement model

$$\mathbf{v}_{k|k-1} = \mathbf{H}[\chi_{k|k-1}]. \quad (20)$$

And predicted measurements from the transformed SPs are calculated as follows

$$\hat{\mathbf{y}}_k^- = \sum_{i=0}^{2L} W_i^{(m)} v_{i,k|k-1}. \quad (21)$$

Then, the observation covariance matrix $\mathbf{P}_{y_k y_k}$ and the cross correlation matrix $\mathbf{P}_{x_k y_k}$ are determined as

$$\mathbf{P}_{y_k y_k} = \sum_{i=0}^{2L} W_i^{(c)} [v_{i,k|k-1} - \hat{\mathbf{y}}_k^-][v_{i,k|k-1} - \hat{\mathbf{y}}_k^-]^T + \mathbf{R}, \quad (22)$$

where \mathbf{R} is the measurement noise covariance matrix.

$$\mathbf{P}_{x_k y_k} = \sum_{i=0}^{2L} W_i^{(c)} [\chi_{i,k|k-1} - \hat{\mathbf{x}}_k^-][v_{i,k|k-1} - \hat{\mathbf{y}}_k^-]^T. \quad (23)$$

The Kalman gain factor is computed via equation of

$$\kappa_k = \mathbf{P}_{x_k y_k} \mathbf{P}_{y_k y_k}^{-1}. \quad (24)$$

At last, the updated states and the covariance matrix are determined by:

$$\hat{\mathbf{x}}_k = \hat{\mathbf{x}}_k^- + \kappa_k (\mathbf{y}_k - \hat{\mathbf{y}}_k^-), \quad (25)$$

$$\mathbf{P}_k = \mathbf{P}_k^- - \kappa_k \mathbf{P}_{y_k y_k} \kappa_k^T. \quad (26)$$

III. FIELD EXPERIMENT RESULTS

In this part, the performance of the integrated INS/GPS system is evaluated for open area application. The results include velocity estimation accuracy analysis during GPS data outages, which are simulated to analyze the system performance in the prediction mode.

The car was driven on the asphalt road during field tests. The vehicle movement trajectory is shown in the Fig. 3. The IMU and GPS receiver were fixed rigidly on a board inside the car. The minimal difference of the orientation of the y-axis (IMU coordinate frame) and gravity vector was achieved by alignment of the board. The tilts angles of the board were carefully verified in order to guarantee required orientation of y-axis. Finally, correct adjustment of the x-axis gives minimal difference of the orientation of the vehicle and IMU coordinate system. The sensors data during experiment was recorded on the HDD of the notebook and then processed using UKF, EKF [8] and KF [9]. Algorithm was implemented using Matlab® software. These data processing algorithms were adjusted in order to guarantee minimal velocity estimation error (RMSE) in the presence of the GPS signal.



Fig. 3. The vehicle movement trajectory on the map.

The estimation of the vehicle velocity, when GPS signal outage occurs during 160 s using KF, EKF and UKF is shown in the Fig. 4. The performance of the considered data processing algorithms will be discussed in more details later.

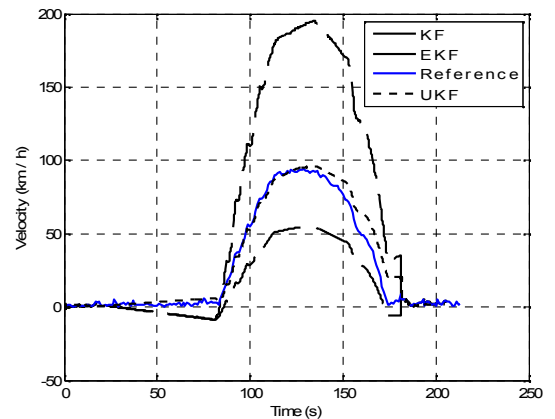


Fig. 4. The vehicle velocity estimation with GPS signal outage during 20 s...180 s.

Now we would like to highlight that the analysed velocity profile contains different types of the vehicle motion: stationary periods during $t \in \{0...82\}s$ and $t \in \{175...198\}s$, high dynamic periods with variable acceleration of the vehicle during $t \in \{82...115\}s$ and $t \in \{137...175\}s$, period with nearly constant vehicle velocity $t \in \{115...137\}s$ (see reference velocity profile in the Fig. 4). The GPS signal outages are simulated during mentioned above time periods of the vehicle moving for the comparative performance analyse of the sensor data processing algorithms. The tuning parameters of data processing algorithms remain identical for each of the analysed GPS signal outage simulation case.

The KF, EKF and UKF performance analysis for stationary mode is given in the Table I. The GPS signal outage time was equal to 60 s for each simulation. Only the starting time for GPS signal outage was different, so that the time period, when the vehicle was in the stationary mode with the presence of the GPS signal, with each next simulation was increased by 5 s. The velocity estimation error (RMSE) continuously decreases (for the EKF and the UKF) with increasing of the initial time of the vehicle stationary mode with the presence of GPS signal. This is correct behavior of the algorithm, which correctly estimates errors of the inertial sensors and adequately models considered here low cost integrated navigation system. As we can see from the Table I, the velocity estimation error was smaller for the UKF algorithm except the cases when the initial time (in this case it is 5 s–6 s) for the UKF algorithm adaptation was not enough.

TABLE I. VELOCITY ESTIMATION ERRORS* DURING GPS OUTAGE.

Period of GPS outage	KF		EKF		UKF	
	RMSE, km/h	ΔV , km/h	RMSE, km/h	ΔV , km/h	RMSE, km/h	ΔV , km/h
5...65 s	20.7	36.0	19.0	33.0	24.3	41.0
6...66 s	9.2	16.0	17.6	31.0	22.0	37.0
10...70 s	6.6	11.0	15.2	26.0	13.1	22.0
15...75 s	13.9	26.0	9.0	18.0	8.0	13.5
20...80 s	6.7	13.5	6.8	13.0	3.5	5.7
21...81 s	15.8	27.0	5.4	10.7	3.3	5.4

Note: *estimation of errors includes RMSE of velocity estimate (RMSE) and absolute maximal estimated velocity error (ΔV) during GPS signal outage.

The velocity estimation errors for high dynamic mode of the vehicle motion are presented in the Table II. Very good performance metrics for the KF, when vehicle was moving with nearly constant velocity, are not surprising, because parameters (acceleration and velocity of the vehicle, accelerometer bias) of the system changes slowly during small GPS signal outage period and hence it can be easily predicted by KF. In all other cases the UKF algorithm considerably outperforms the KF and the EKF algorithms. The rather high value of the velocity estimation error (RMSE) by the UKF for GPS signal outage during 120 s...180 s can be explained by the fact that the GPS outage period starts quite quickly after high dynamic mode of the car motion. This doesn't allow for the UKF to stabilize state estimates.

The velocity estimation error (for KF, EKF, UKF) reaches

maximum (ΔV) in the end of GPS signal outage period, when the car was in stationary mode or moving with nearly constant velocity, but that's not necessarily the case, when the car was moving with variable acceleration.

TABLE II. VELOCITY ESTIMATION ERRORS* DURING GPS OUTAGE.

Period of GPS outage	KF		EKF		UKF	
	RMSE, km/h	ΔV , km/h	RMSE, km/h	ΔV , km/h	RMSE, km/h	ΔV , km/h
20...120 s	40.8	95.0	20.2	41.0	3.3	5.7
120...180 s	33.3	74.0	18.2	33.0	7.3	11.0
20...180 s	60.1	103.0	23.6	41.0	8.1	20.0
116...136 s	3.24	7.0	5.9	10.0	5.4	7.0
120...130 s	3.1	5.0	1.7	2.8	2.1	2.5

Note: *estimation errors include RMSE of velocity estimate (RMSE) and absolute maximal estimated velocity error (ΔV) during GPS signal outage.

IV. CONCLUSIONS

The comparative performance analysis of UKF, EKF and KF for the car velocity estimation was performed for different dynamic mode of the vehicle movement during GPS signal outages.

The UKF algorithm adapted for the low cost sensors data processing has smaller velocity estimation error during GPS signal outages comparing with EKF algorithm. This is especially obvious for the cases when vehicle has experienced quick changes in the dynamics of car movement. Also, the velocity estimation error (RMSE) is weakly dependent from the average and top speed of the car.

The next step of this research should be devoted to the definition of the optimal tuning parameters of the UKF algorithm for the different car motion scenarios.

REFERENCES

- [1] A. Priyanka, S. Zainab, N. Aboelmagd, El-Sheimy Naser, *MEMS-Based Integrated Navigation*. London: Artech House, 2010, pp. 1–62.
- [2] V. Bistrov, "Study of the characteristics of random errors in measurements by MEMS inertial sensors", *Automatic Control and Computer Sciences*, vol. 45, no. 5, pp. 284–292, 2011. [Online]. Available: <http://dx.doi.org/10.3103/S0146411611050051>
- [3] H. Garcia de Marina, F. Espinosa, C. Santos, "Adaptive UAV Attitude Estimation Employing Unscented Kalman Filter, FOAM and Low-Cost MEMS Sensors", *Sensors*, vol. 12, pp. 9566–9585, July 2012. [Online]. Available: <http://dx.doi.org/10.3390/s120709566>
- [4] Zhou Jianjun, Song Chunlei, Zhuang Huihui, "Square root unscented Kalman filter for MEMS gyroscope random drift compensation", *Journal of Central South University (Science and Technology)*, vol. 42, no. 1, pp. 469–472, Sep. 2011.
- [5] S. Haykin, *Kalman filtering and neural network*. New York, USA: John Wiley & Sons, Inc., 2001, pp. 221–253. [Online]. Available: <http://dx.doi.org/10.1002/0471221546>
- [6] R. Van Der Merwe, E. A. Wan. "Sigma-point particle filters for sequential probabilistic inference in dynamic state-space models", *Proc. of the Int. Conf. On Acoustics, Speech, and Signal Proc. IEEE*. Hong Kong, 2003.
- [7] P. D. Groves, *Principles of GNSS, Inertial, and Multisensor Integrated Navigation Systems*. London: Artech House, 2008, pp. 97–145.
- [8] V. Bistrov, A. Kluga, "Adaptive extended Kalman filter for aided inertial navigation system", *Elektronika ir elektrotechnika (Electronics and Electrical Engineering)*, no. 6, pp. 37–40, 2012.
- [9] V. Bistrov, "Analyse of Kalman algorithm for different movement modes of land mobile object", *Elektronika ir elektrotechnika (Electronics and Electrical Engineering)*, no. 6, pp. 89–92, 2008.